Design optimization and image reconstruction for position sensitive thermal neutron detectors with ANTS2 toolkit

Andrey Morozov, *Luis Margato, Alberto Blanco, Raimundo Martins* (LIP-Coimbra)

Irina Setefanescu (ESS)

Karl Zeitelhack (FRM-II)

PSND-2018 Julich, May 15-17

ANTS2 highlights

ANTS2 targets PSSDs development and focuses on:

- Fast prototyping and optimization of design
- Optimization of position reconstruction techniques
- Light response model reconstruction
- Image reconstruction

ANTS2 highlights

Simulations

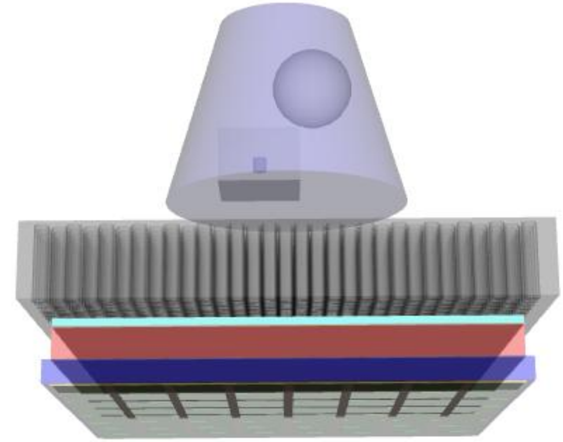

- 3D, custom detector geometry
  (based on TGeoManager of CERN ROOT)
- Generation and tracking of gamma rays,
  neutrons and charged particles (not electrons!)
- Primary and secondary scintillation
- Tracing of optical photons
- Photon scattering, wavelength shifters
- Signal generation for PMTs and SiPMs

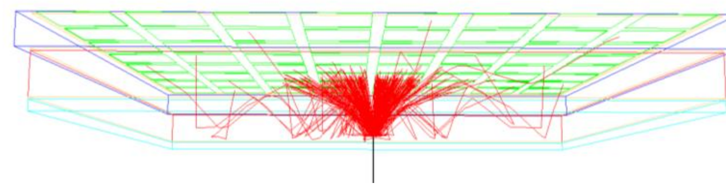

Event reconstruction (XYZ + energy)

- Statistical reconstruction algorithms
- Real-time capable (GPU-based) reconstruction
- Artificial neural network and kNN-based
  reconstruction

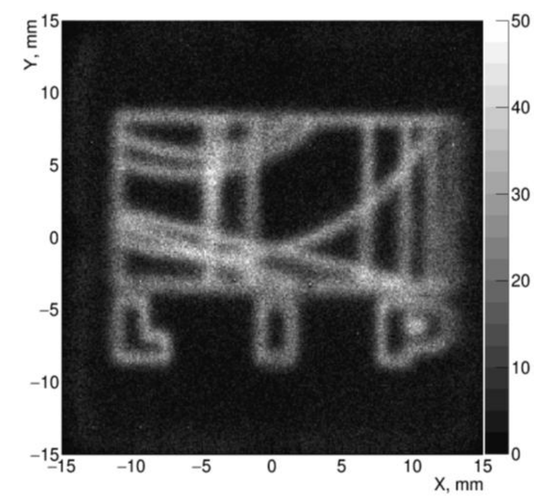

Neutrons in ANTS2

- Materials: gas mixtures of the corresponding isotopes (T = 300K)
- Elastic scattering is considered without coherent effects
  - Scattering is isotropic in the center of mass frame (isotope + neutron)
- Isotope velocities are sampled directly from the Maxwell distribution without correction for the Doppler effect

- Total elastic (N,EL) and total non-elastic (N,NON) cross-sections vs energy from the ENDF/B-VII.1 database
  - JEFF-3.2 and JENDL-4.0u2 databases for missing data

Comparison with Geant4

Geant4 version 4.9.6.p02

QGSP_BIC_HP physics list (G4NeutronHP model)
Cross-sections from ENDF/B-VI.1 (JEFF and JENDL for missing data)

Float glass slab of 100 x 100 x 0.5 mm^3
Composition: SiO_2 : 72.98 + Na_2O : 14 + CaO : 7 + MgO : 4 + Al_2O_3 : 2 + K_2O : 0.02

Mono-energetic (25.3 meV) neutrons enter the slab through the centre of the "In" face of the slab (normal direction)

	Geant4	**ANTS2**
Total # of incoming neutrons	$1 \cdot 10^7$	$1 \cdot 10^7$
Passed without interactions	9 871 793	9 871 448
Scatter -> forward	68 233	67 274
Scatter -> sides	145	92
Scatter -> back	55 731	56 261
Absorbed	4098	4057

Comparison with Geant4

Energy distributions of the neutrons exiting the slab faces

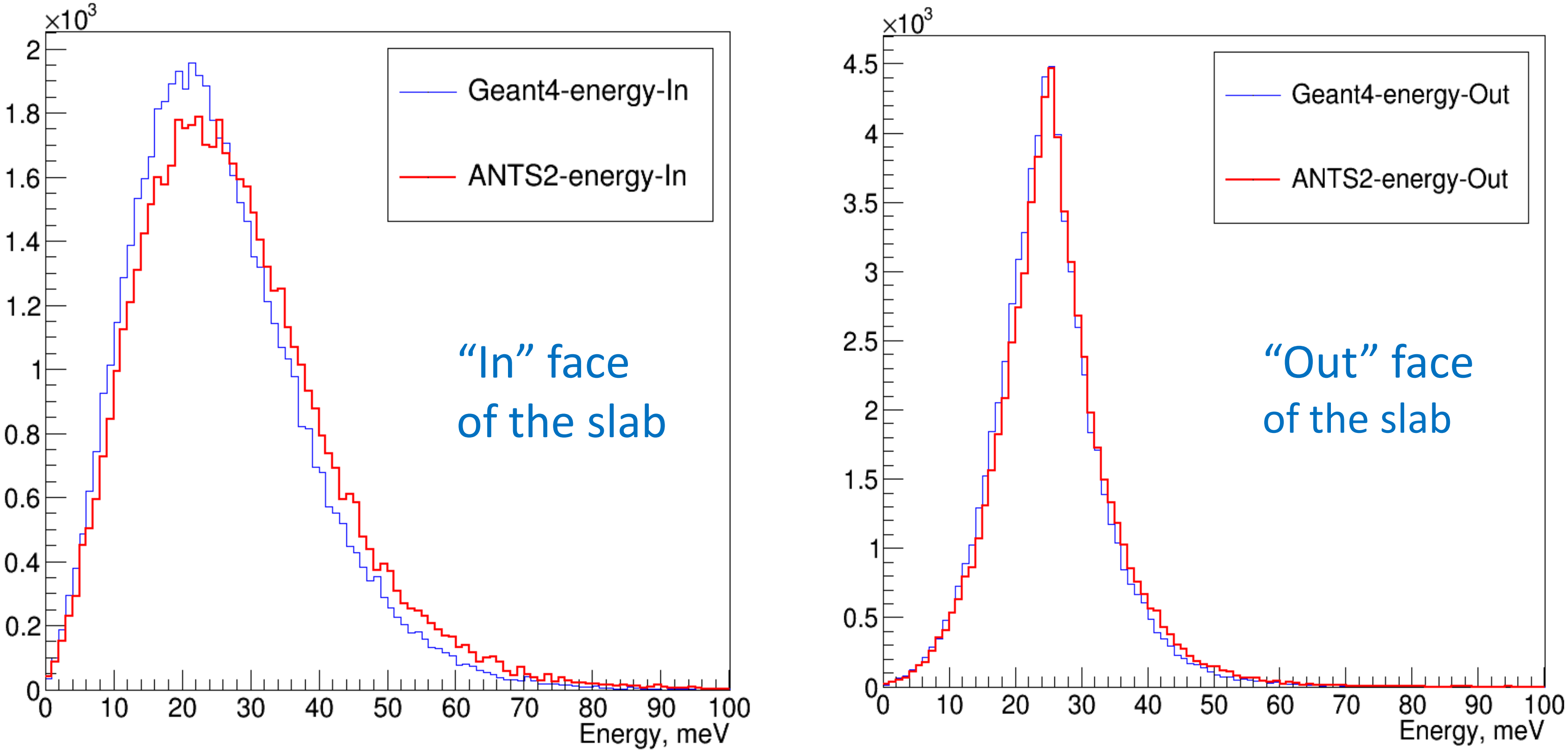

Comparison with Geant4

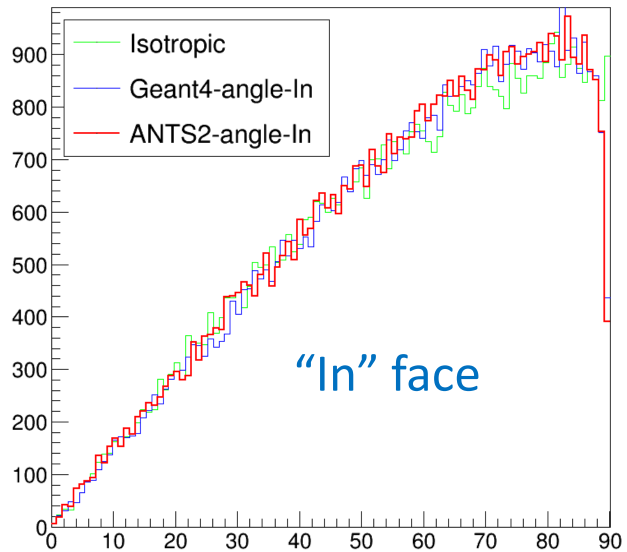

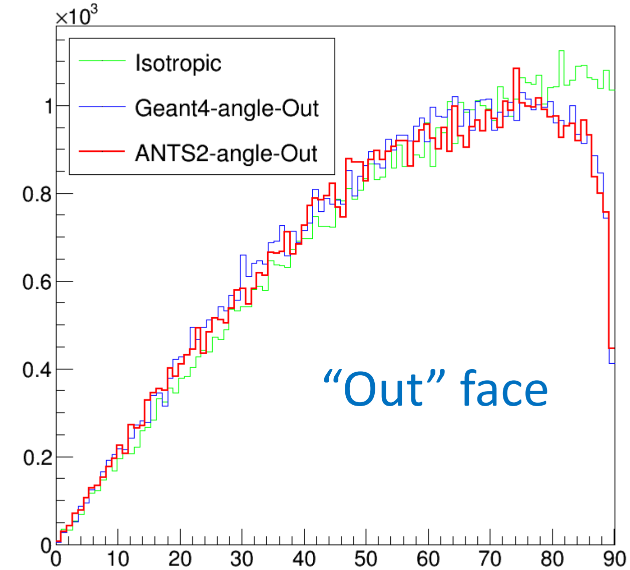

Distribution of the exit angles

For comparison, isotropic distribution (green) is also shown

Spatial distribution of the **exit positions** over the "**Out**" face:

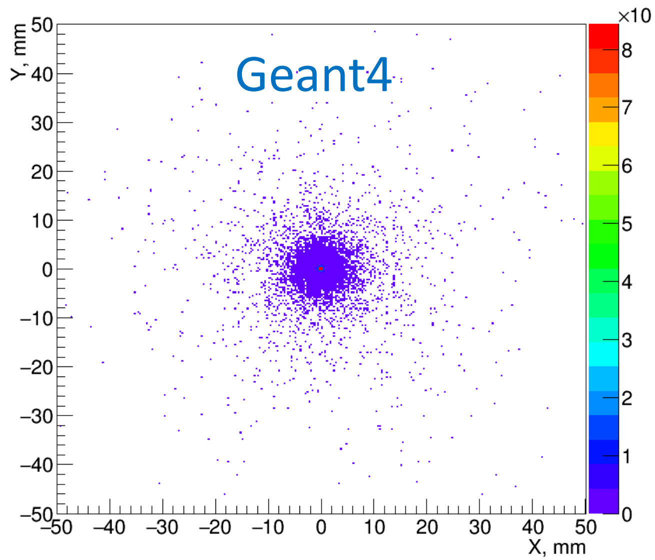

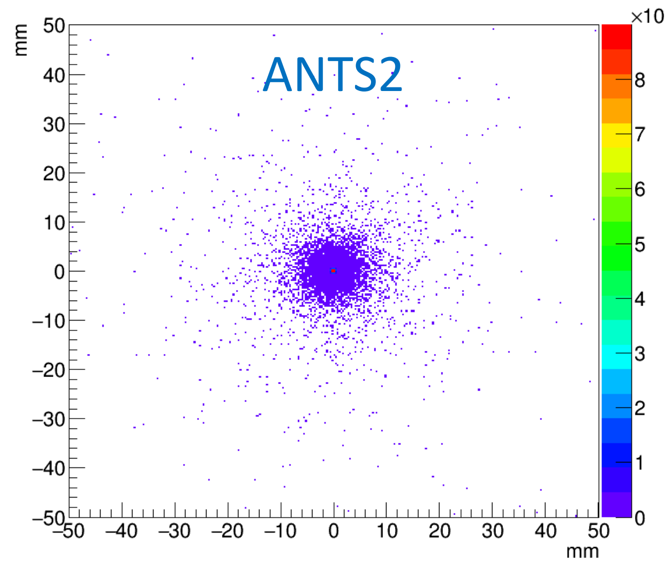

Compact GS20 camera

64 SiPMs with individual readout, 30 x 30 mm^2 GS20 scintillator + lightguide

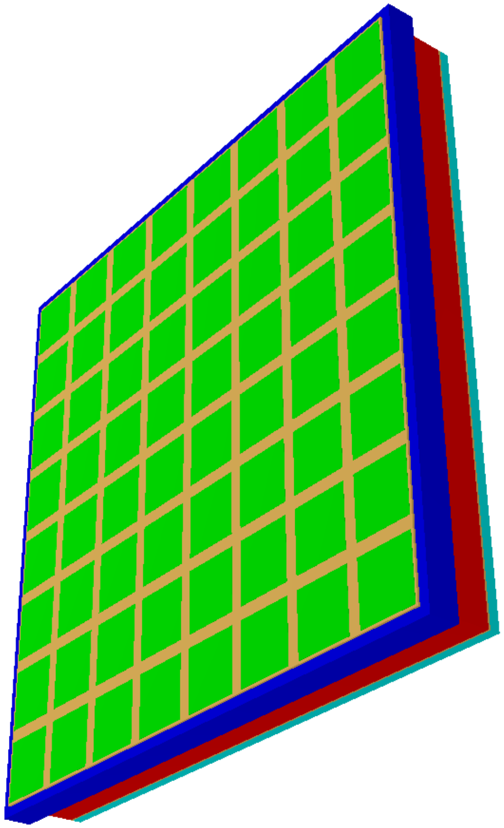

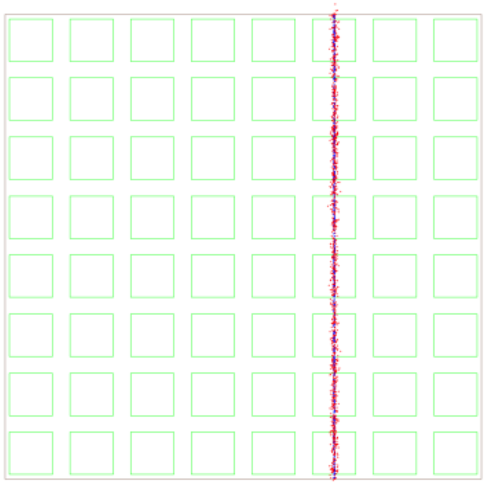

Simulation: Potential to reach 0.5 mm spatial resolution

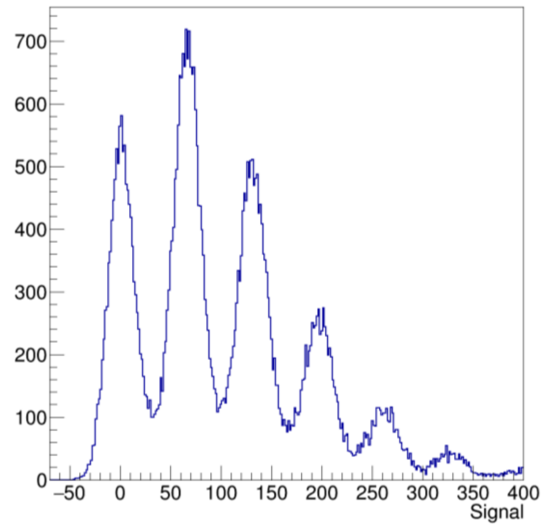

Simulation of **SiPM signals** (dark counts, optical cross-talk, electronic noise)

Compact GS20 camera

Statistical reconstruction of event position and energy

Auto-calibration capabilities:
requires only flood irradiation data for camera calibration

Simulation:

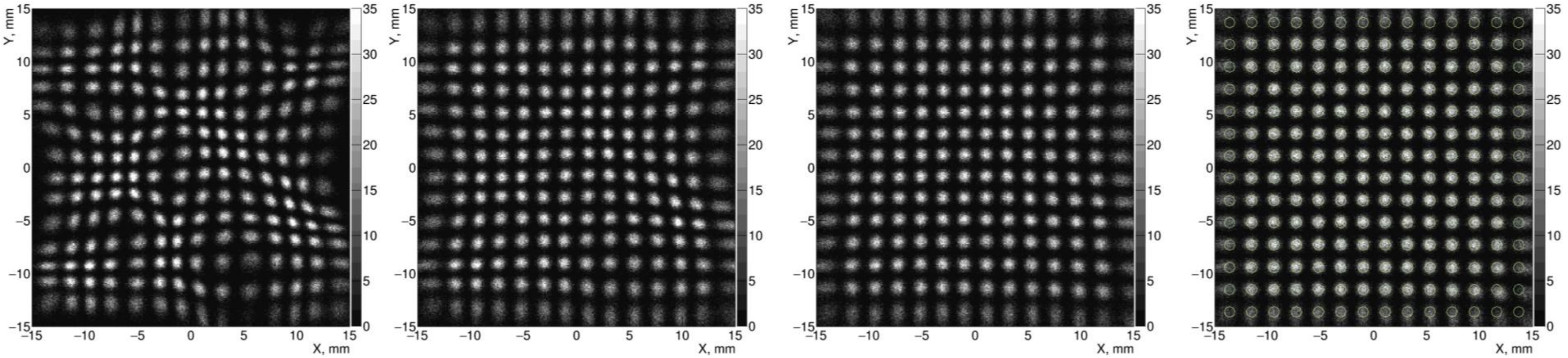

Flood field dataset is used for iterative reconstruction of the detector response

Pencil beam scan dataset is used to demonstrate the improvement of the camera responce model with iterations (0th, 1st, 4th and 20th)

For gamma camera: A Morozov *et al* 2017 *Phys. Med. Biol.* **62** 3619

Detector with WSF

Diffuse scintillator, covered with reflective layer +
wavelength shifting fibers +
SiPMs with the **fiber couplers**:

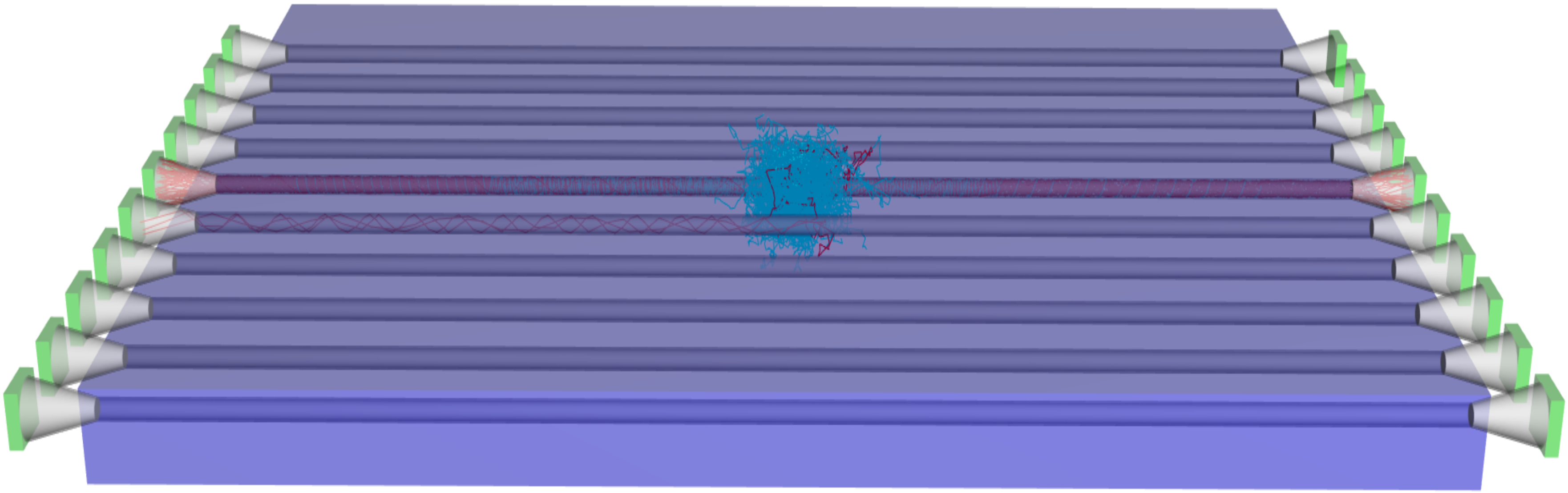

“Tracks”:

Red – photons reaching the SiPMs

Teal – the rest of the photons

Detector with WSF

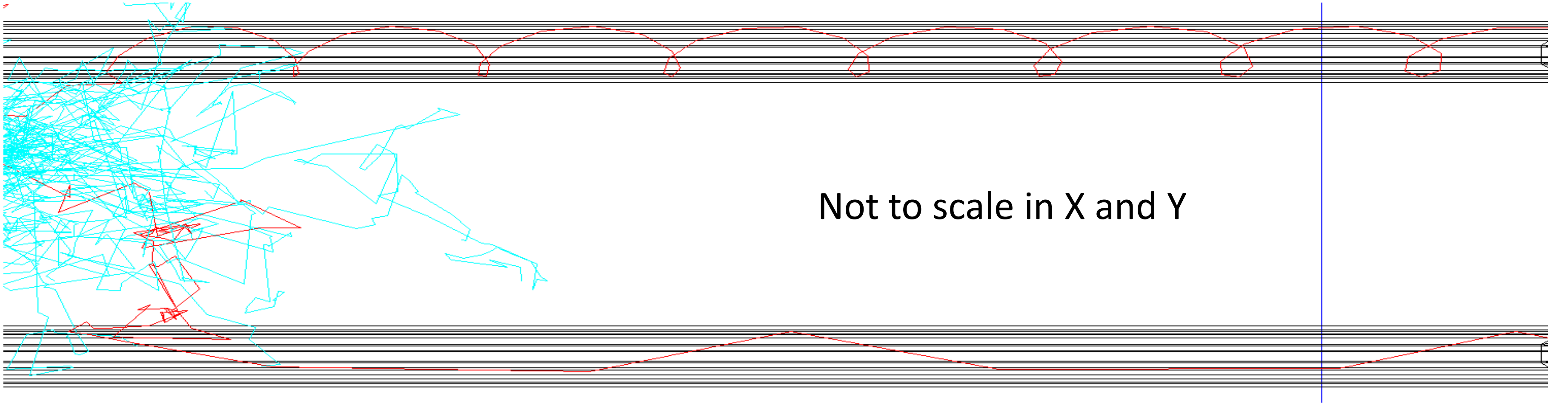

Scintillation:
point source (75 mm from the plane of the left and 25 mm from the plane of the right SiPMs)

Distribution of the distances inside the fiber cores:
Red – photons detected by the left SiPMs
Blue – photons detected by the right SiPMs

Data analysis performed using the ***photon*** scripting unit of ANTS2

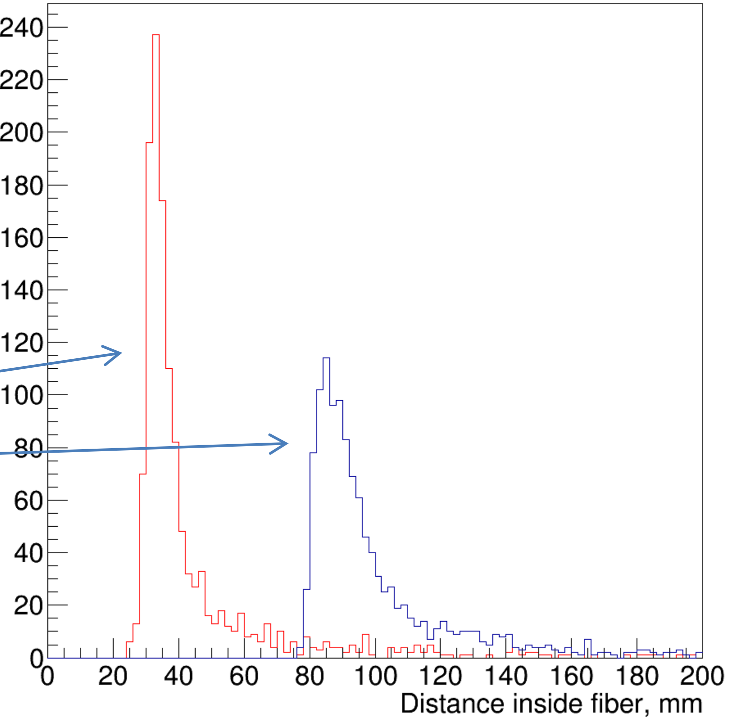

RPC-based detectors

10-double-gap RPC detector

3D view:

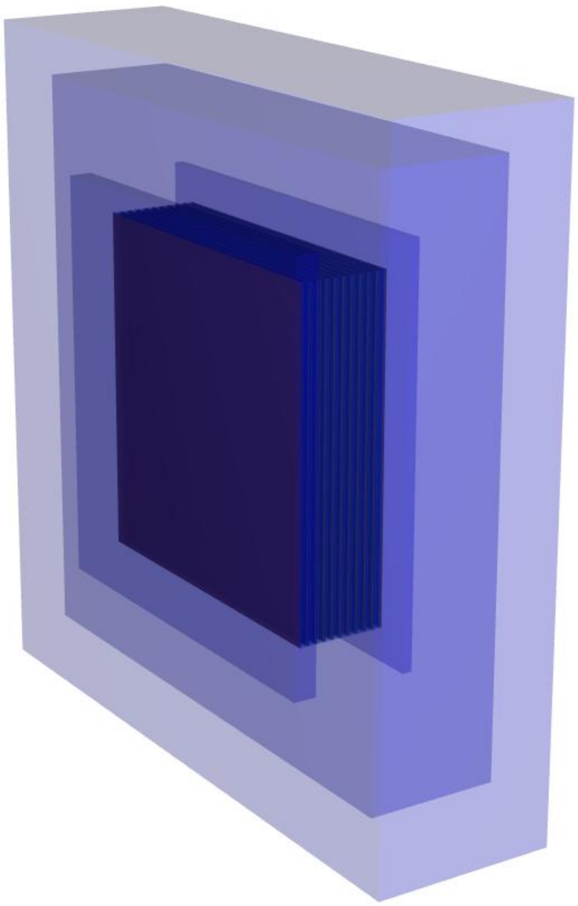

Side parallel view, stretched in Y:

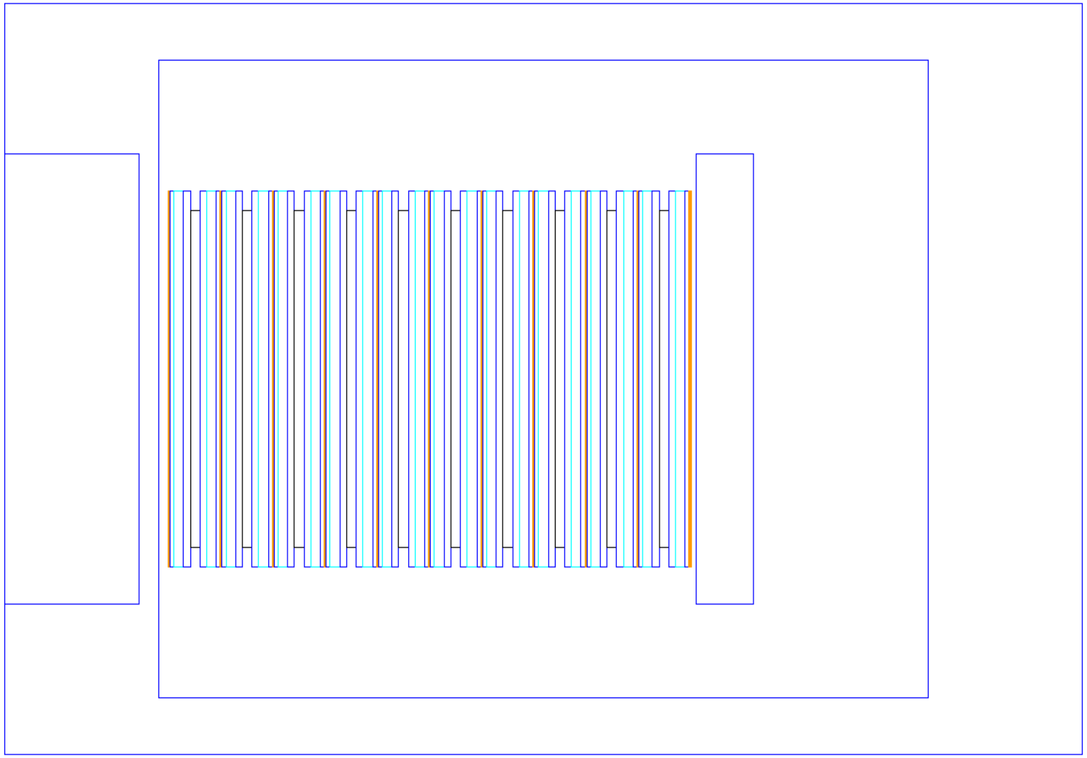

RPC detectors

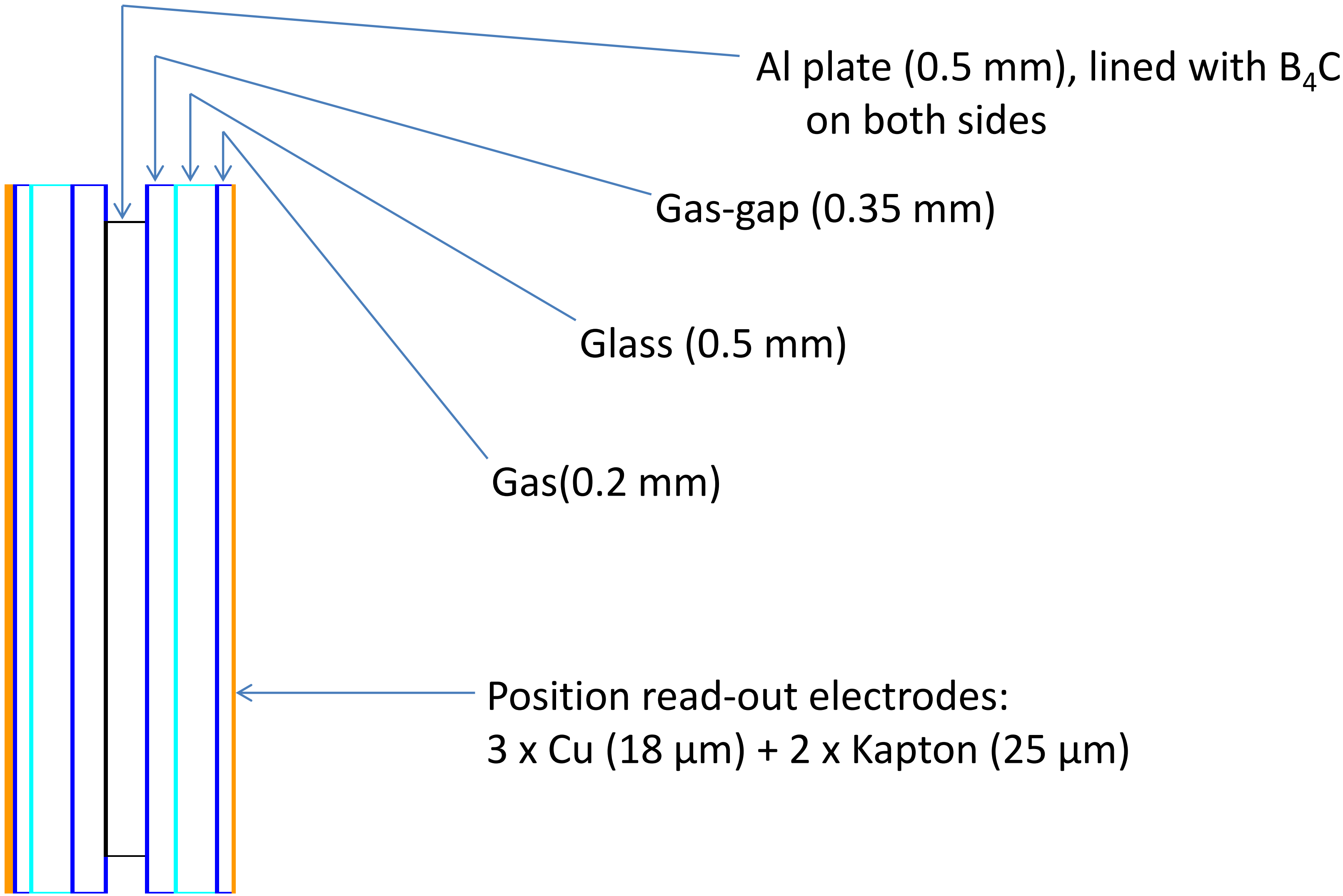

Detection efficiency (DE)

1) **All converters are 1.15 µm thick** (as the prototype tested at FRM-II)

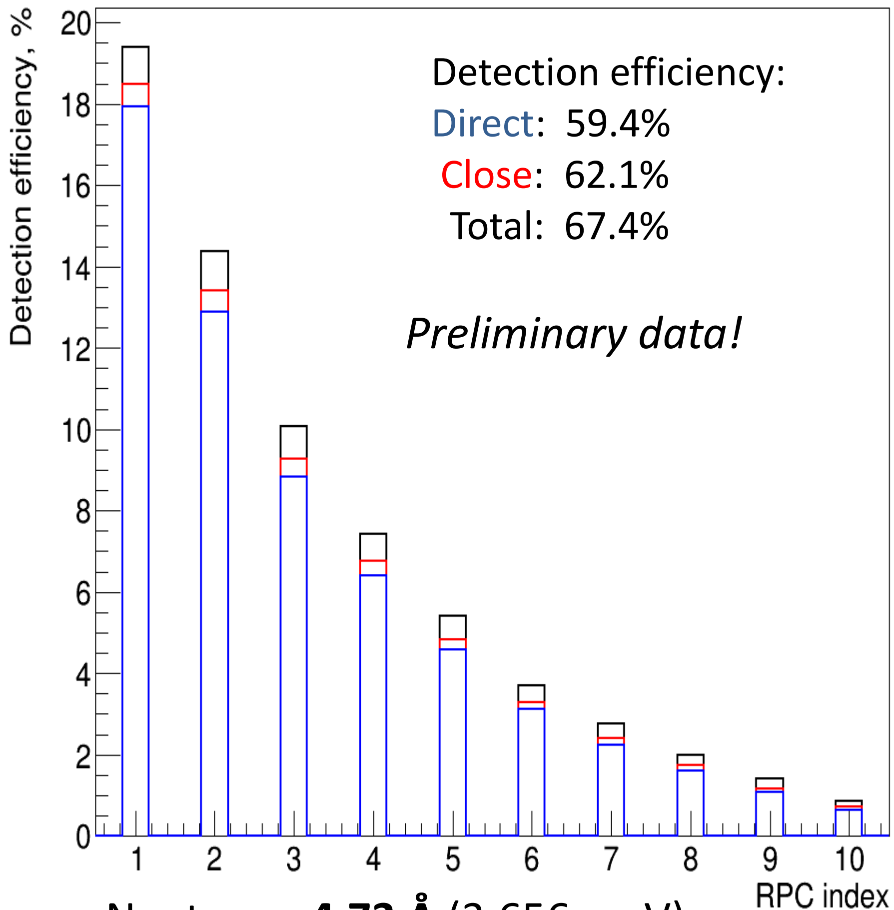

Neutrons: **4.73 Å** (3.656 meV)
10 keV threshold

Absorption probability: 93%

Direct DE - detection efficiency for neutrons without prior scattering

Close DE - the fragment (α or ^{7}Li) enters the gas gap with X and Y < 0.5 mm from the neutron pencil beam axis

Total DE - all detected events

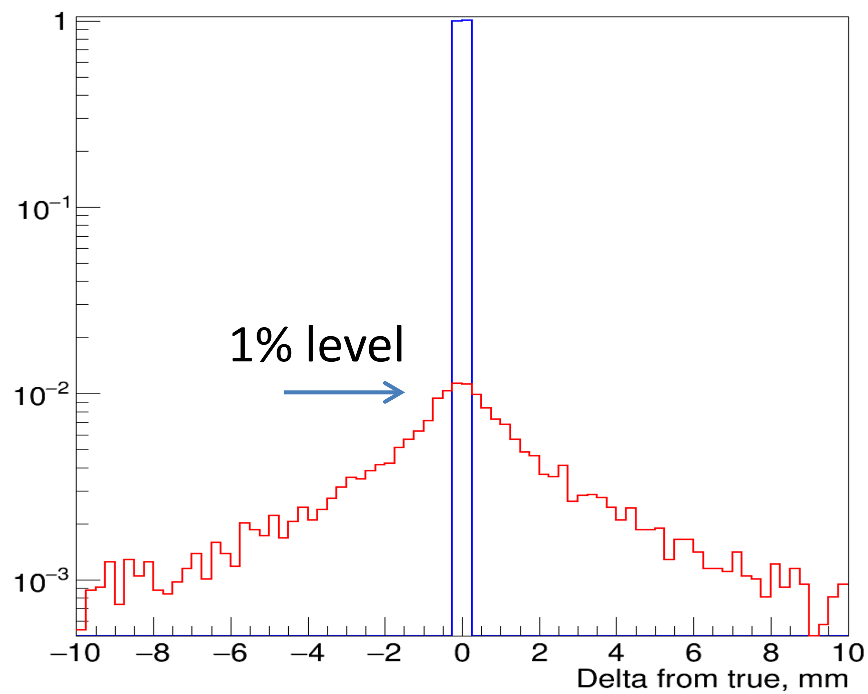

RPC detectors: Optimization

2) Conditional optimization:

a) the total detection efficiency as high as possible

b) the count rates of all RPCs as equal as possible

Also, from practical considerations:

c) only five different B_4C thicknesses

1 1 2 2 3 3 3 3 4 4 4 4 4 4 5 5 5 5 5 5 (ordered by RPC#)

Maximization parameter:

Close DE multiplied by the *equality* parameter: $P = \frac{\sum_{i=1}^{n} E_i}{n E_m}$

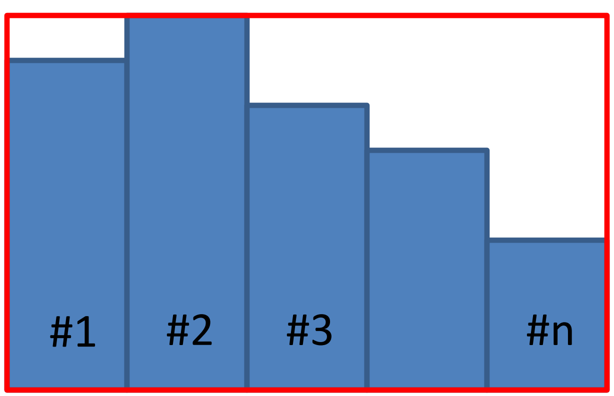

P is the ratio of the "Blue" and "Red" areas

RPC detectors: Optimization

Best result (n=10): converter thicknesses of 0.34, 0.39, 0.47, 0.74 and 1.94 μm

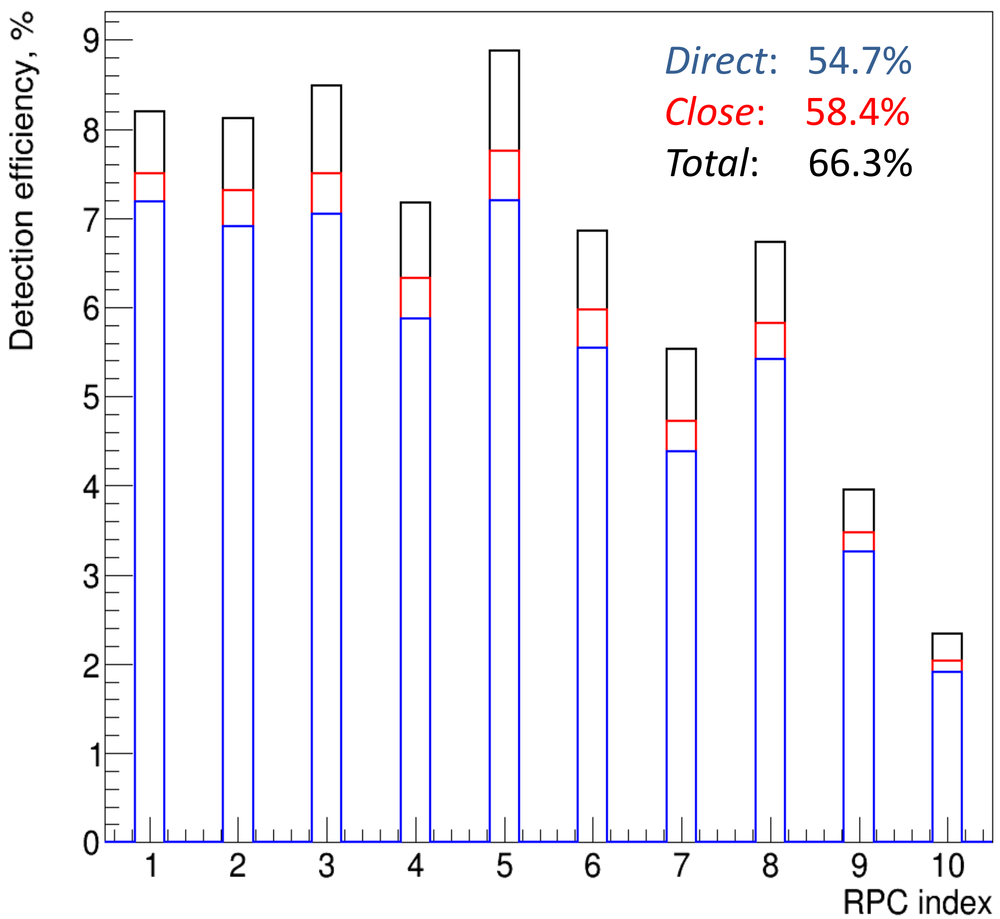

Much better distribution over the RPCs!

But the price is:

4% less in the *close* DE compared to the case of equal thicknesses

x2 more scattering

RPC detectors: Optimization

RPCs	*Close* detection efficiency		Thicknesses, um	
	total, %	by layers, %		
3	43.0	14.6, 14.7, 13.7	0.77/1.12/2.95	P2
3	41.8	13.7, 14.0, 14.1	0.71/1.0/2.30	I'
4	49.6	13.7, 13.9, 12.6, 9.4	0.71/1.00/1.47/2.15	P2
4	47.5	11.9, 11.9, 12.6, 11.1	0.60/0.76/1.16/1.81	P2
4	48.5	12.5, 12.7, 12.2, 11.0	0.64/0.84/1.18/2.08	I'
5	54.6	12.2, 11.9, 12.2, 10.7, 7.6	0.61/0.77/1.10/1.60/2.26	P2
5	53.9	10.3, 12.5, 12.5, 10.8, 7.7	0.49/0.79/1.11/1.65/2.26	I'
6	56.0	9.5, 10.0, 10.2, 10.2, 9.3, 6.8	0.44/0.57/0.76/1.01/1.34/1.72	P2
6	58.7	11.7, 12.5, 12.5, 9.8, 7.2, 5.0	0.59/0.78/1.19/1.34/1.58/1.83	I'
6	54.5	9.5, 9.6, 9.7, 9.7, 9.6, 6.4	0.43/0.54/0.68/0.88/1.31/1.22	I''
7	59.6	7.9, 9.5, 10.1, 10.3, 9.4, 7.4, 5.1	0.36/0.50/0.68/0.92/1.2/1.5/1.9	P2
7	58.8	8.2, 9.2, 9.1, 8.9, 9.2, 8.2, 6.0	0.38/0.49/0.59/0.74/1.04/1.6/2.4	P3
7	59.8	9.0, 9.9, 9.6, 9.9, 9.0, 7.8, 4.7	0.41/0.54/0.64/0.92/1.2/2.1/2.1	I'''
8	57.4	6.4, 6.7, 7.3, 8.1, 8.1, 8.0, 7.0, 5.9	0.29/0.33/0.42/0.54/0.71/0.91/1.1/1.4	P2
8	60.0	6.8, 8.2, 8.4, 8.4, 8.2, 8.0, 7.0, 5.0	0.30/0.43/0.52/0.62/0.78/1.1/1.6/2.3	P3

P2 n-th layer thicknesses as $a_0 + a_1 \cdot n + a_2 \cdot n^2$
P3 n-th layer thicknesses as $a_0 + a_1 \cdot n + a_2 \cdot n^2 + a_3 \cdot n^3$
I Individual minimization (# of parameters = # of RPCs)

Minimization parameter: *Close* D.E. multiplied by ***P***

RPC detectors: Materials

20 double-gap RPC, 1.15 µm converter thickness

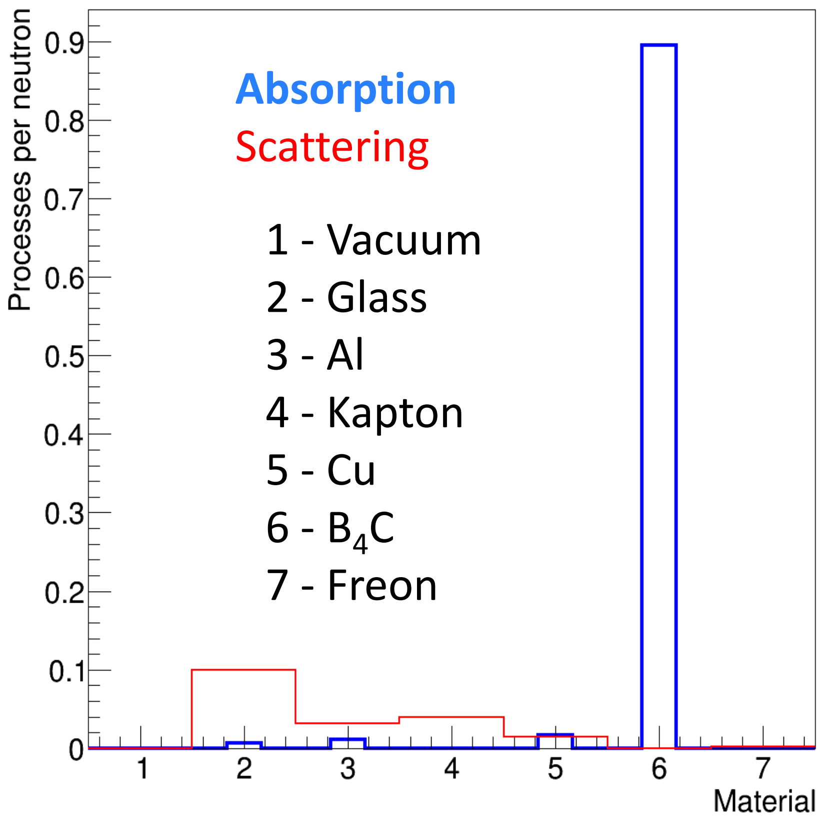

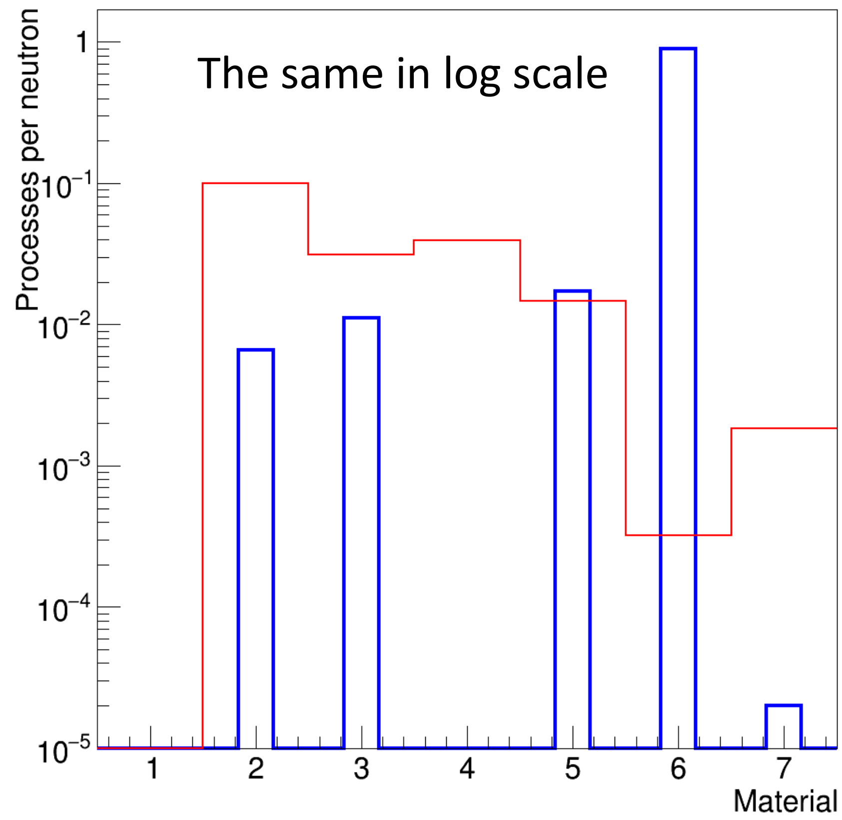

Absorption probability: 93%; Proability of at least one scattering: 15%

RPC detectors: Optimization

Next generation detector prototype (10 double-gap RPCs):

Glass: 0.5 → 0.35 mm
Al plates: 0.5 → 0.3 mm
Kapton: 2 → 1 plate
Electrodes: Cu → Al

Optimization with the same method results in:

0.32, 0.40, 0.46, 0.65 and 2.00 μm layers
Direct / *close* / *total* DE: 60.7% / 63.5% / 69.1%

For comparison:

Rate-optimized previous generation: 54.7% / 58.4% / 66.3%
Prototype with 1.15 μm thicknesses: 59.4% / 62.1% / 67.4%

Absorption: Total probability 89%; with no prior scattering 78%

Scattering: Probability of at least one scattering 16.5% (1: 14% 2: 2% 3: 0.4%)
By material: glass 63%, Al 21%, Kapton 16%

Simulations *vs* experiment

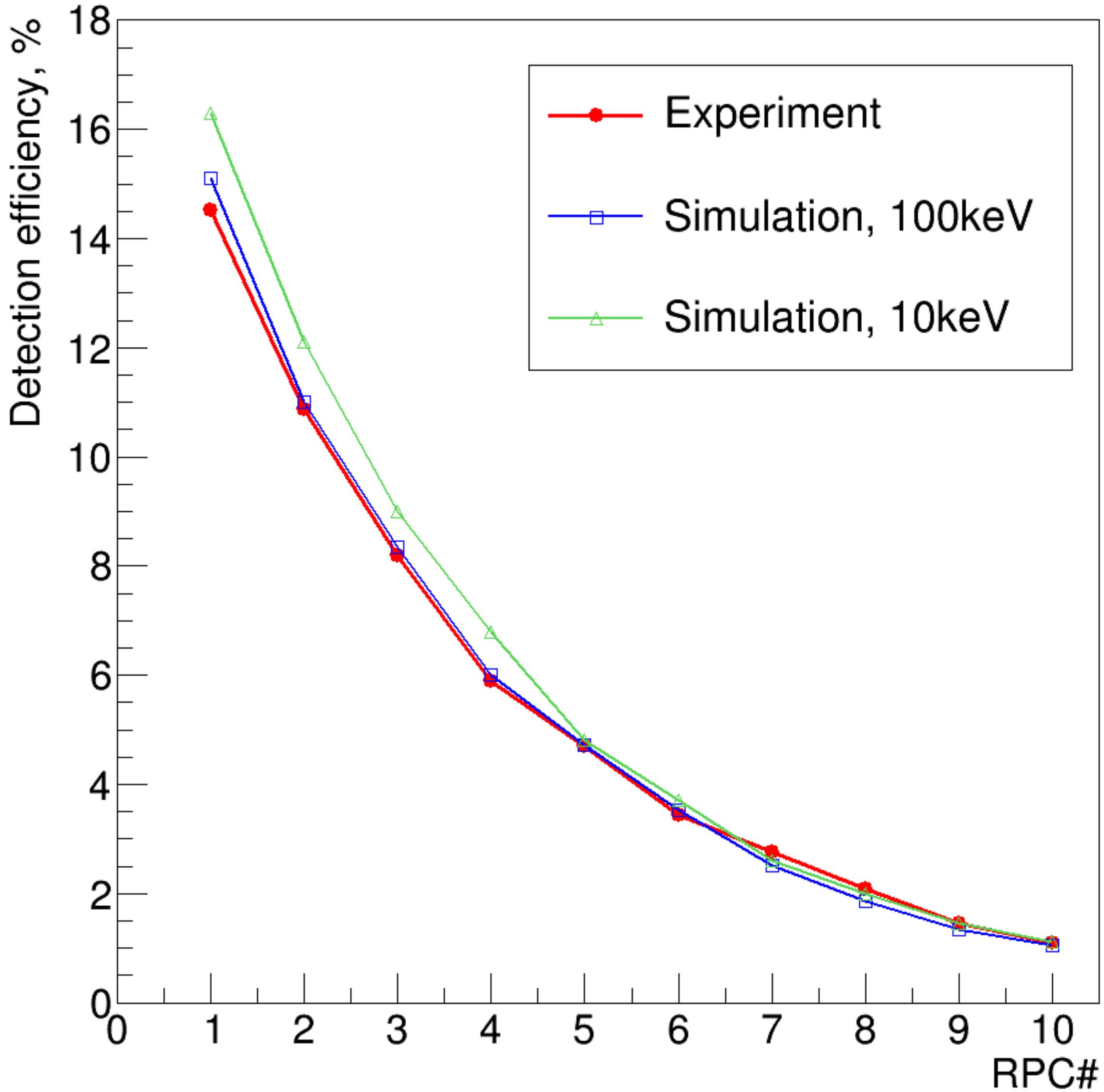

Experiment:
The prototype with 1.15 μm converters at the TREFF beamline at FRM-II.
RPC HV is 2300V
Calibration: ^{3}He tube.

Simulations:
10 and 100 keV deposition threshold for neutron to be detected;
Refined detector model

RPC detectors: Image uniformity

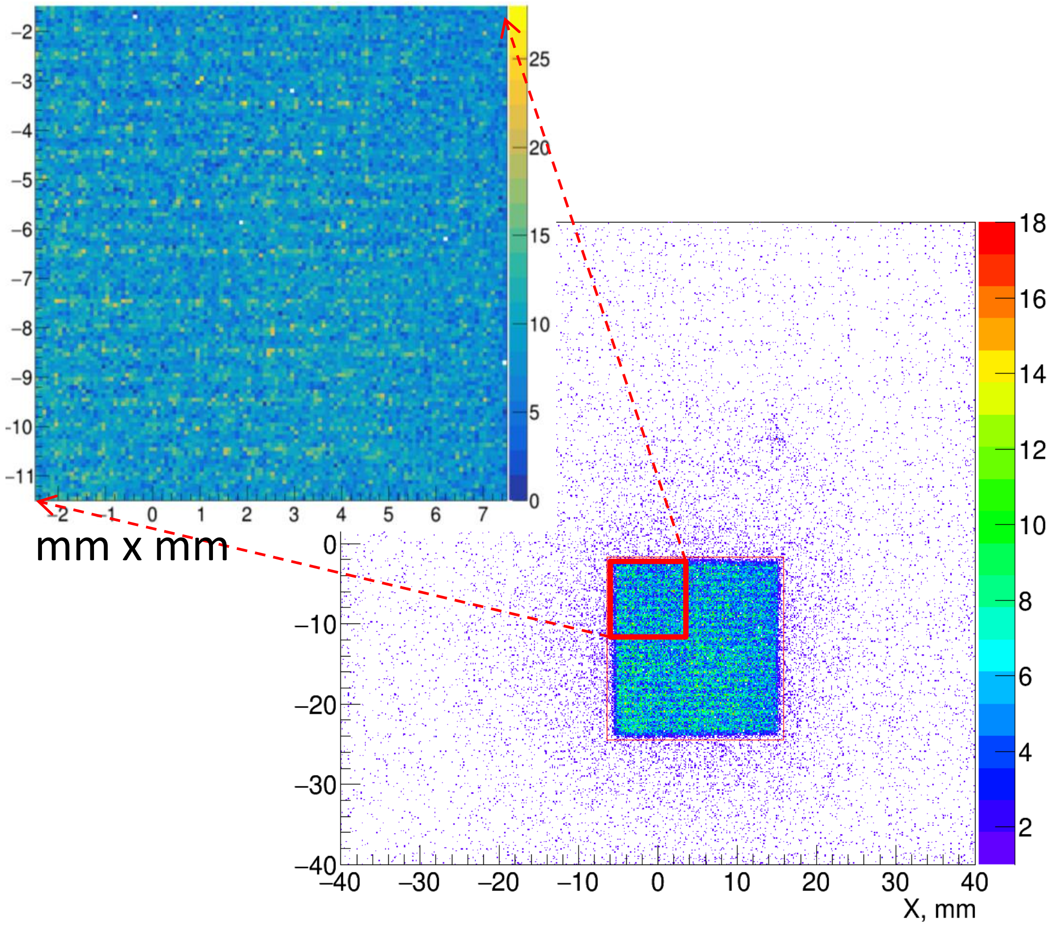

Centroid (**CoG**) reconstruction + sum signal filters

Pattern period is 0.5 mm
Pitch of the pads is 1 mm

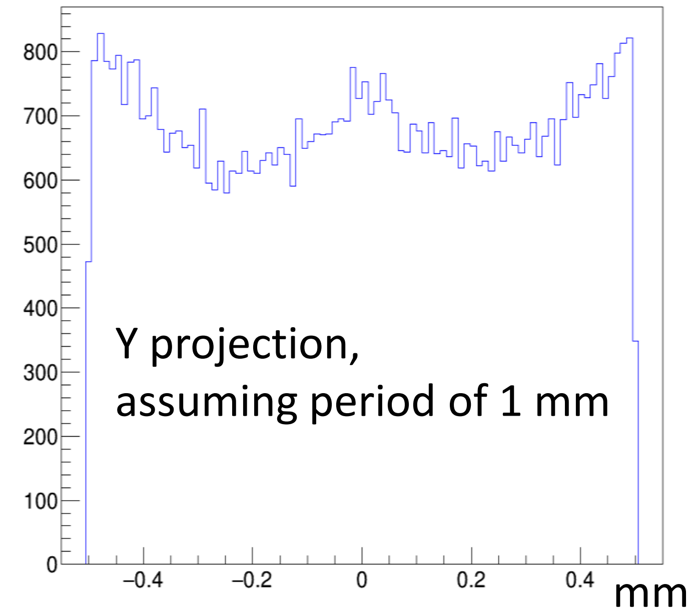

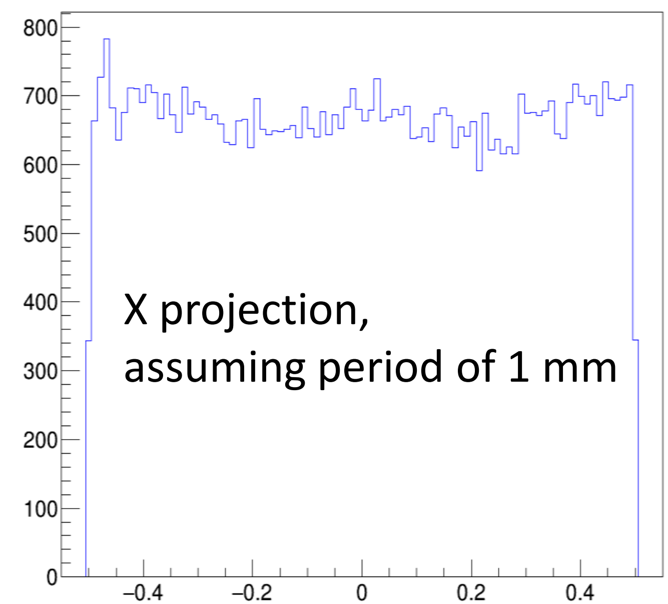

RPC detectors: PRF

Pad Response Function (PRF) – average pad signal as a function of the projection of the distance between the reconstruction position and the pad center.

Very rough estimation of the PRF in Y direction using CoG reconstruction and smoothing:

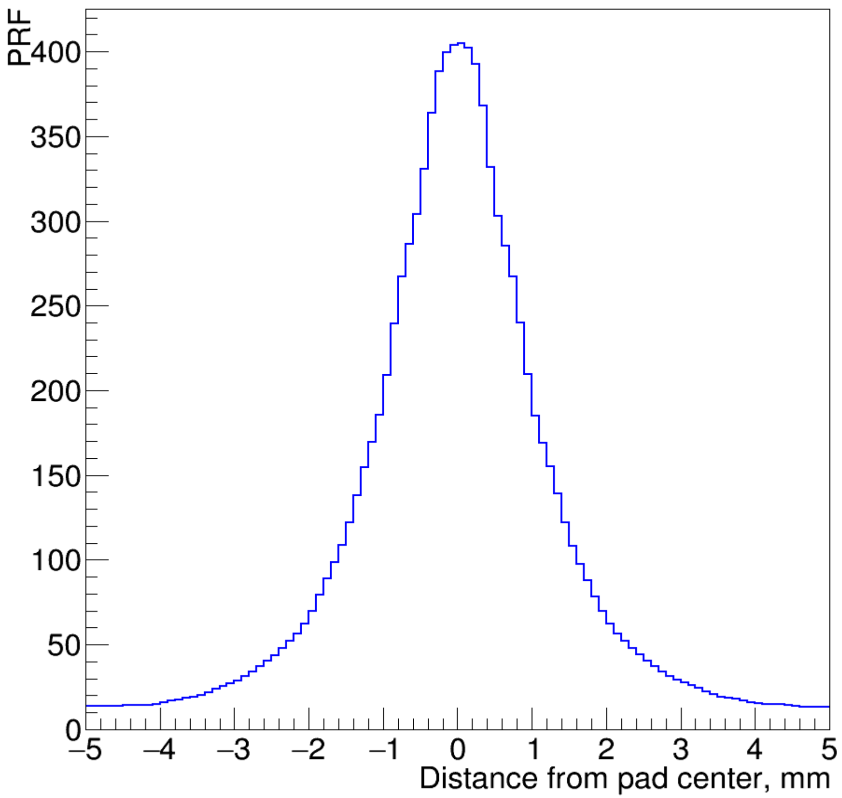

Maximum observed multiplicity is 8 (pad pitch is 1 mm)

It is likely that statistical reconstruction is feasible!

Next experimental campaign:
need experimental datasets with a fine scan using narrow slit!

RPC detectors: CoG

Mock simulation:

- Events positions are randomly distributed over a ractangular area
- Pad signals are generated using the same PRF (no fluctuations!)
- CoG reconstruction

Y reconstructed *vs* Y true (Pads centers are at ... -1.5, -0.5, 0.5, 1.5 ... mm)

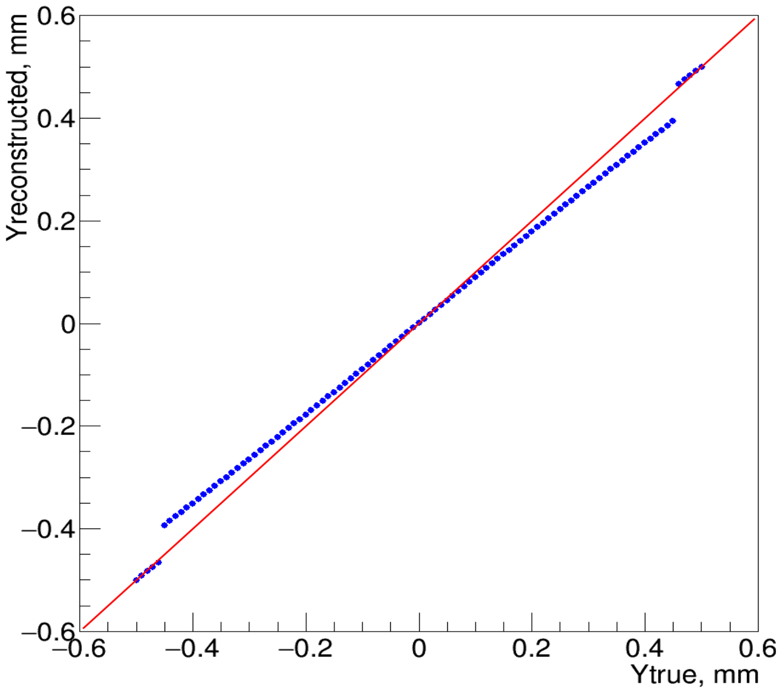

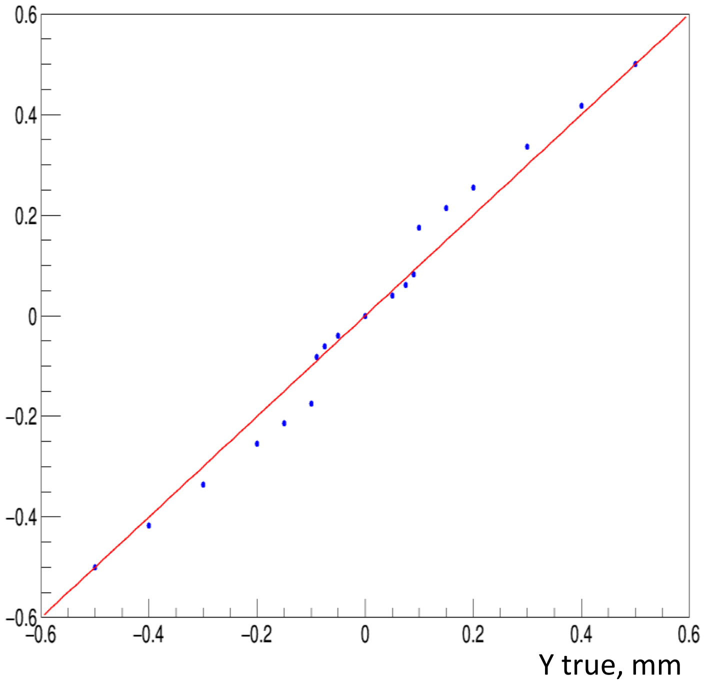

With PRF from the previous slide

With PRF estimated assuming Lorenzian profile

RPC detectors: CoG

Non-uniformity in CoG-reconstructed images:

1) Due to CoG intrinsic distortions

Can be corrected with a LUT

2) Discreteness of pads

Limited number of the pads used

or suppression of signal < threshold:

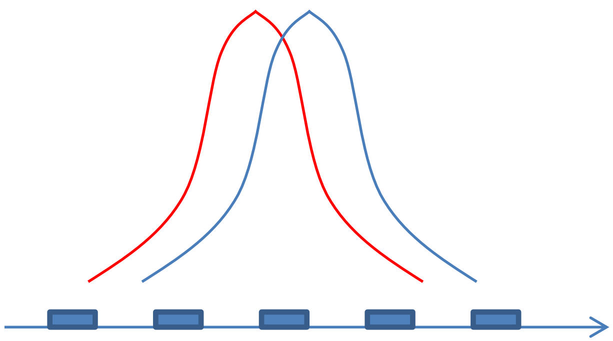

LUT approach can be inefficient due to energy dependence of the “jumps” in reconstruction!

Better to replace CoG with, e.g., a statistical reconstruction method.

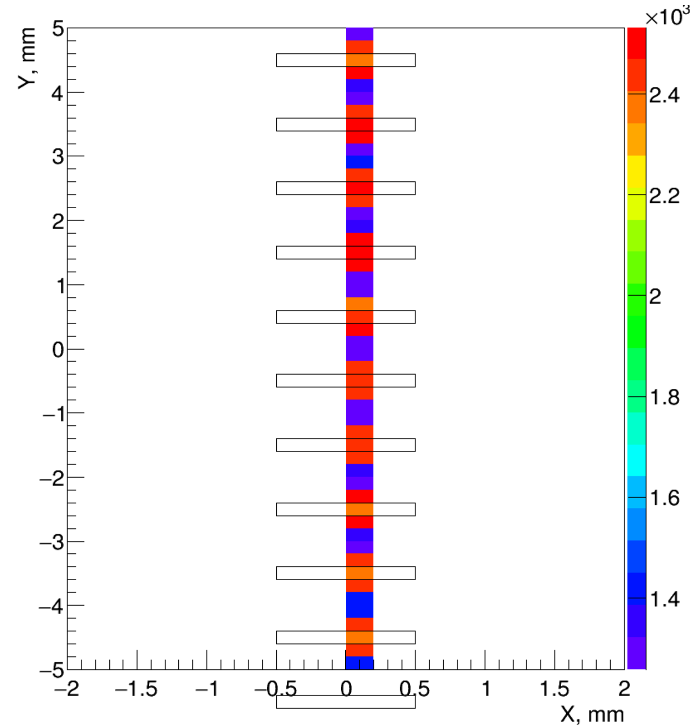

Density of reconstructed events (colour-coded) using the result of the mock simulation (previous slide, Lorenzian profile)

Next step: try to apply itrative response reconstruction developed for 2D PSSDs

ANTS2 implementation details

ANTS2 is written in C++ using Qt framework
Requires installation of CERN ROOT
Scripting: JavaScript, Python (work in progress)

Optional libraries:

EIGEN3:	for fast LRF/PRF fitting
CUDA toolkit:	for GPU-based statistical reconstruction
FANN:	for ANN reconstruction
FLANN:	for kNN reconstruction and event filtering

ANTS2 runs on Linux and Windows,
probably on Mac too - no one tried hard enough :)

Open source and more detailed information can be found at:

https://github.com/andrmor/ANTS2
http://coimbra.lip.pt/ants/ants2

Use Dev branch!